PASJ: Publ. Astron. Soc. Japan **61**, 1261–1269, 2009 December 25

Viscous Accreting Magnetofluids around a Static Compact Object in Final Stages of Accretion Flow

Jamshid GHANBARI and Mahboobeh SHAGHAGHIAN
Department of Physics, School of Sciences, Ferdowsi University of Mashhad, Mashhad, Iran
ghanbari@ferdowsi.um.ac.ir, m.shaghaghian@fsriau.ac.ir, m.shaghaghian@gmail.com

(Received 2009 February 10; accepted 2009 August 10)

Abstract

The dynamics of the stationary axisymmetric configuration of accreting magnetofluids surrounding a non-rotating compact object in the final stages of accretion flow is presented here. We discuss two classes of solutions for the angular momentum: a Keplerian solution, which demands no accretion flow for the fluids, and a non-Keplerian solution, which requires a radial inflow velocity for the matter. For the special case of no presence of electromagnetic fields, two sets of self-consistent analytical solutions of fully relativistic fluid equations are obtained separately for two different equations of state. The effect of the bulk viscosity coefficient on the physical functions was investigated for each state, as well as the bounds that exert on the free parameters due to last stages of the accretion-flow condition. To resolve the magnetohydrodynamical equations, we were inspired by previous sets of solutions, since the magnetofluid equations are just the same as the fluid ones in the case of vanishing electromagnetic fields. The azimuthal current in magnetofluids doesn't modify the dipolar configuration of the central object magnetic field, owing to the lack of a finite resistivity. The presence of this magnetic field doesn't affect the azimuthal velocity of the plasma, but does slow down its radial inflow, and decrease the density and pressure of the plasma. Despite the role importance of the bulk viscosity on the fluids' dynamics in the absence of electromagnetic fields, exerting the magnetic field decreases this role.

Key words: accretion — general relativity — magnetohydrodynamics

1. Introduction

The plasma processes in the vicinity of compact objects are believed to be the main mechanisms for the generation of energy in them. Falling matter releasing gravitational potential energy heats the gas, and generates radiation. The process of angular-momentum removal of the infalling material operates on slower time-scales as compared to the free-fall time, so infalling gas with sufficiently high angular momentum can form a disk-like structure around a central gravitating body. All accretion-flow models require that the angular momentum be removed from the flow in some way so that material can flow inwards. If the velocity field varies significantly in directions orthogonal to the flow (shearing motions), shear viscous effects come into play (Frank et al. 1992). Shear viscosity, which is an angular-momentum transport mechanism, operates on a finite time-scale of τ_v. It becomes equal to or larger than the accretion time-scale, τ_{acc}, as the accreted material approaches the horizon, before the final plunge (Peitz & Appl 1997). Consequently, neglecting the shear viscosity is a wise assumption during the last stages of accretion flow, while most of the gas orbital angular momentum has already been removed and the fluids' radial inflow is several times faster than its rotation.

Studies of the axisymmetric stationary magnetofluid configuration around compact objects in context of high-energy astrophysics are of long-standing considerable theoretical interest in both Newtonian and relativistic limits (e.g., Kaburaki 1986; Tripathy et al. 1990; Takahashi et al. 1990; Banerjee et al. 1995, 1997; Ghosh 2000; Tomimatsu & Takahashi 2001). If the gravitational field is sufficiently strong, as in the vicinity of a compact object, the Newtonian description of gravity is only a rough approximation, and general-relativistic considerations are necessitated. In studying the relativistic disks, there are two kinds of assumptions about the self-gravity of the disks. One is to assume that the self-gravity is the source of space-time curvature, and to refer to solve Einstein's field equations (Lynden-Bell & Pineault 1978; Cai & Shu 2002). The other idea is that the self-gravity is negligible compared to the gravitation of the central compact object, and it is assumed that the basic geometry just produced by the central object is not disturbed by the self-gravity of the disk (Prasanna 1989; Takahashi et al. 1990; Kudoh & Kaburaki 1996; Gammie & McKinney 2003; Antón et al. 2006). The basic equations governing the dynamics of an axisymmetric stationary magnetofluid disk around a compact object in curved space-time are given by Prasanna et al. (1989). Considering the viscosity, in those equations p changes to $\overline{p} = p - (\eta_b - \frac{2}{3}\eta_s)\Theta$ (Prasanna & Bhaskaran 1989; Bhaskaran & Prasanna 1990; Peitz & Appl 1997; Banerjee et al. 1997; Riffert 2000). Prasanna (1989) demonstrated that an initial spherical matter accretion (i.e., accretion with initial zero angular momentum and radially falling at infinity) onto a rotating black hole may acquire angular velocity entirely due to inertial frame dragging induced by the space-time surrounding the compact object as it approaches the horizon, and forms a thin disk structure on the equatorial plane of the central compact object before the final plunge. In this scenario, the pressure balance at a marginally stable orbit is provided by the equality of the radiation pressure and the hydrostatic gas

pressure. Furthermore, the bulk viscosity does contribute in the dynamical equations through the nonzero radial velocity. The existence of such solutions of exact equations gives us sufficient motivation to study the dynamics of accreting fluids around a non-rotating compact object during the last moments of accretion flow. We take up a study of the dynamics of a disk-like structure around a static compact object in final stages of accretion flow. Once the specific angular momentum of the gas is small enough in such a way that in those instants, the accretion flow more nearly resembles the free-fall on to the central compact object. Namely, it is assumed that an accretion disk had previously been formed in the gravitational field surrounding a non-rotating compact object. We would now like to investigate the fluids' dynamical treatments during the last stages of accretion flow for two different equations of state in two cases, while the electromagnetic fields are present and not; also, the role of the bulk viscosity on the dynamics is considered for each case.

This paper is organized as follows: In section 2, the governing basic equations are derived according to special assumptions. Observing the equations of state to close the system of equations is carried out in section 3. For the special case of no magnetic field being present, two sets of self-consistent analytical solutions for two different equations of state can be found in section 4, and numerical solutions for magnetofluid case are described in section 5. Conclusions and possible generalizations are presented in section 6.

2. Basic Equations

The general system that we shall consider is viscous magnetofluids surrounding a non-rotating compact object. We ignore a very slow increase in the mass of the central object due to accretion. The space-time produced by the central compact object is introduced by the Schwarzschild geometry, and then the fluids are supported entirely by the object's gravitational field. The line element of the space-time is written as

$$ds^2 = \left(1-\frac{2m}{r}\right)c^2dt^2 - \left(1-\frac{2m}{r}\right)^{-1}dr^2 - r^2\left(d\theta^2+\sin^2\theta d\varphi^2\right), \tag{1}$$

where c is the light speed, $m = GM/c^2$ is the Schwarzschild mass, M denotes the mass of the central compact object and G is the gravitational constant. The energy-momentum tensor for an imperfect magnetofluid is given by

$$T^{ij} = \left(\rho+\frac{\bar{p}}{c^2}\right)u^iu^j - \frac{\bar{p}}{c^2}g^{ij} + \frac{2}{c^2}\eta_s\sigma^{ij} - \frac{1}{4\pi c^2}\left(F^i_{\ k}F^{jk} - \frac{1}{4}g^{ij}F_{kl}F^{kl}\right), \tag{2}$$

with $\bar{p} = p - (\eta_b - \frac{2}{3}\eta_s)\Theta$ and $\Theta = u^k_{\ ;k}$ is invariant. Here, ρ, p, η_b and η_s denote the mass density, gas pressure, bulk and shear viscosity coefficients, respectively.

$$\sigma^{ij} = \frac{1}{2}(u^{i;k}h^j_{\ k} + u^{j;k}h^i_{\ k}) - \frac{1}{3}\Theta h^{ij}, \tag{3}$$

being the shear tensor wherein $h^{ij} = g^{ij} - u^iu^j$ is the projection tensor. Note that the Roman indices run from 0 to 3 and the Greek ones run from 1 to 3. The governing magneto-hydrodynamical equations are obtained (Prasanna et al. 1989) by considering the conservation laws,

$$T^{ij}_{\ ;j} = 0, \tag{4}$$

along with the following Maxwell equations:

$$\begin{aligned} &F^{ij}_{\ ;j} = -\tfrac{4\pi}{c}J^i, \\ &F_{ij,k} + F_{ki,j} + F_{jk,i} = 0. \end{aligned} \tag{5}$$

We are interested in expressing the dynamical equations in the orthonormal tetrad frame appropriate to the Schwarzschild metric,

$$\lambda^i_{(\alpha)} = \mathrm{diag}\left[\left(1-\frac{2m}{r}\right)^{-1/2}, \left(1-\frac{2m}{r}\right)^{1/2}, \frac{1}{r}, \frac{1}{r\sin\theta}\right]; \tag{6}$$

all variables are then defined in local Lorentz frame as follows:

$$\begin{aligned} F_{(\alpha)(\beta)} &= \lambda^i_{\ (\alpha)}\,\lambda^j_{\ (\beta)}F_{ij}, \\ J^{(\alpha)} &= \lambda^{(\alpha)}_{\ i}J^i, \\ E_{(\alpha)} &= F_{(\alpha)(t)}, \\ B_{(\alpha)} &= \epsilon_{\alpha\beta\gamma}F_{(\beta)(\gamma)}, \end{aligned} \tag{7}$$

where $\epsilon_{\alpha\beta\gamma}$ is the Levi–Civita symbol. Using the same tetrad, the spatial 3-velocity, V^α, defined through the relation $u^\alpha = u^0V^\alpha/c$, in terms of local Lorentz components are given by

$$\begin{aligned} V^{(r)} &= \left(1-\frac{2m}{r}\right)^{-1}V^r, \\ V^{(\theta)} &= r\left(1-\frac{2m}{r}\right)^{-1/2}V^\theta, \\ V^{(\varphi)} &= r\sin\theta\left(1-\frac{2m}{r}\right)^{-1/2}V^\varphi. \end{aligned} \tag{8}$$

The Maxwell equations in this coordinates are then written as

$$\begin{aligned} &\frac{\partial}{\partial\theta}\left(\sin\theta\ B_{(\varphi)}\right) = -\frac{4\pi r}{c}\sin\theta J^{(r)}, \\ &\frac{\partial}{\partial r}\left[r\left(1-\frac{2m}{r}\right)^{1/2}B_{(\varphi)}\right] = \frac{4\pi r}{c}J^{(\theta)}, \\ &\frac{\partial}{\partial r}\left[r\left(1-\frac{2m}{r}\right)^{1/2}B_{(\theta)}\right] - \frac{\partial B_{(r)}}{\partial\theta} = -\frac{4\pi r}{c}J^{(\varphi)}, \\ &\left(1-\frac{2m}{r}\right)^{1/2}\frac{\partial}{\partial r}[r^2\sin\theta E_{(r)}] + \frac{\partial}{\partial\theta}[r\sin\theta E_{(\theta)}] = -\frac{4\pi}{c}r^2\sin\theta J^{(t)}, \\ &\frac{\partial}{\partial r}\left[r^2\sin\theta B_{(r)}\right] + \frac{\partial}{\partial\theta}\left[r\left(1-\frac{2m}{r}\right)^{-1/2}\sin\theta\ B_{(\theta)}\right] = 0, \\ &\frac{\partial}{\partial r}\left[r\left(1-\frac{2m}{r}\right)^{1/2}E_{(\theta)}\right] - \frac{\partial E_{(r)}}{\partial\theta} = 0, \\ &\frac{\partial}{\partial r}\left[r\left(1-\frac{2m}{r}\right)^{1/2}\sin\theta\ E_{(\varphi)}\right] = 0, \\ &\frac{\partial}{\partial\theta}\left[\sin\theta\ E_{(\varphi)}\right] = 0. \end{aligned} \tag{9}$$

With the assumption of an insignificant toroidal electric field ($E_\varphi = 0$), one admissible solution set of the Maxwell equations (9) is

$$\begin{aligned} E_{(r)} &= E_0 \left(\frac{R}{r}\right)^3 \cos\theta, \\ E_{(\theta)} &= \frac{E_0}{2}\left(\frac{R}{r}\right)^3 \left(1-\frac{2m}{r}\right)^{-1/2} \sin\theta, \\ B_{(r)} &= B_0 \left(\frac{R}{r}\right)^3 \cos\theta, \\ B_{(\theta)} &= \frac{B_0}{2}\left(\frac{R}{r}\right)^3 \left(1-\frac{2m}{r}\right)^{1/2} \sin\theta, \\ B_{(\varphi)} &= \frac{b_\varphi}{r\sin\theta}\left(1-\frac{2m}{r}\right)^{-1/2}, \end{aligned} \tag{10}$$

which gives rise to the following currents:

$$\begin{aligned} J^{(r)} &= 0, \\ J^{(\theta)} &= 0, \\ J^{(\varphi)} &= \frac{-3mc}{4\pi}\frac{B_0}{r^2}\left(\frac{R}{r}\right)^3 \sin\theta, \\ J^{(t)} &= \frac{-2mc}{4\pi}\frac{E_0}{r^2}\left(\frac{R}{r}\right)^3 \left(1-\frac{2m}{r}\right)^{-1/2} \cos\theta. \end{aligned} \tag{11}$$

Here, R represents the radius of the compact object, with B_0 and E_0 being the surface field strengths, and b_φ is an arbitrary constant. Because of the vanishing of the radial and meridional currents, the toroidal magnetic field doesn't appear in the equations. Thus, without any loss of generality, we set $b_\varphi = 0$ (Prasanna et al. 1989). It is assumed that the matter distribution and electromagnetic fields are stationary ($\partial_t \equiv 0$) and axisymmetric ($\partial_\varphi \equiv 0$). Also, it is supposed that there is no meridional flow ($V^\theta = 0$), and the fluids are settled near the equatorial plane of the central object ($\theta = \pi/2$) (Tripathy et al. 1990; Kudoh & Kaburaki 1996) and the system's physical functions are independent of θ. Thus, with these assumptions, the conservation equations can be written as a continuity equation,

$$\left(\rho + \frac{\bar{p}}{c^2}\right)\left[\frac{dV^{(r)}}{dr} + \frac{2}{r}V^{(r)}\right] + V^{(r)}\frac{d}{dr}\left(\rho - \frac{\bar{p}}{c^2}\right) = \frac{3m}{4\pi c^2}\frac{B_0^2}{r^2}\left(\frac{R}{r}\right)^6 V^{(r)}, \tag{12}$$

a radial component,

$$\begin{aligned} &\left(\rho + \frac{\bar{p}}{c^2}\right)\left(1-\frac{V^2}{c^2}\right)^{-1}\left[V^{(r)}\frac{dV^{(r)}}{dr}\right. \\ &\left. + \frac{mc^2}{r^2}\left(1-\frac{2m}{r}\right)^{-1}\left(1-\frac{(V^{(r)})^2}{c^2}\right) - \frac{(V^{(\varphi)})^2}{r}\right] \\ &+ \frac{d\bar{p}}{dr} + \frac{3m}{8\pi}\frac{B_0^2}{r^2}\left(\frac{R}{r}\right)^6 = 0, \end{aligned} \tag{13}$$

and an azimuthal component of momentum equation,

$$V^{(r)}\frac{dV^{(\varphi)}}{dr} + \frac{1}{r}\left(1-\frac{2m}{r}\right)^{-1}\left(1-\frac{3m}{r}\right)V^{(\varphi)}V^{(r)} = 0. \tag{14}$$

Here, $V^{(r)}$, being the radial inflow velocity, is assumed to be positive, which indicates the direction toward the central object. There are two classes of solutions for this set of equations (12)–(14):

(i) There is no accretion flow, or $V^{(r)} = 0$. In this case, equations (12) and (14) are satisfied identically. Also, one can assume the quasi-Keplerian form for the toroidal component of the velocity field (Banerjee et al. 1997) as being

$$V^{(\varphi)} = \sqrt{\left(1-\frac{2m}{r}\right)^{-1}\frac{GM}{r}}. \tag{15}$$

With this value of $V^{(\varphi)}$, the centrifugal force is completely balanced by the gravitational force, and thus the pressure gradient needed to balance the magnetic stress is

$$\frac{d\bar{p}}{dr} = -\frac{3m}{8\pi}\frac{B_0^2}{r^2}\left(\frac{R}{r}\right)^6. \tag{16}$$

The class (i) solutions indicate the outer regions where the radial inflow velocity is so slow. Prasanna et al. (1989) has elaborately discussed this class of solution.

(ii) The second class, which is more important for us, is achieved by omitting $V^{(r)}$ from equation (14); then, a first-order homogeneous differential equation is obtained, which is resolved simply as

$$V^{(\varphi)} = \frac{L}{r}\left(1-\frac{2m}{r}\right)^{1/2}, \quad l = \frac{L}{cm}, \tag{17}$$

where L is an integration constant, and l is called the angular-momentum parameter. As a result, once the centrifugal force is no longer balanced by the gravitational force, rather it is smaller than the inward gravitational attraction, radial inflow will occur for the matter. The transition radius, r_{tr}, between these two classes of solutions in the initial and middle instants of accretion flow is obtained by the matching condition,

$$V^{(\varphi)}_{\text{keplerian}}\,|_{r=r_{tr}} = V^{(\varphi)}_{\text{radial inflow}}\,|_{r=r_{tr}}, \tag{18}$$

which leads to the following equation:

$$\left(1-\frac{2m}{r_{tr}}\right)\sqrt{\frac{m}{r_{tr}}} = \frac{1}{l_{tr}}, \tag{19}$$

and / or

$$x_{tr}^{3/2} = l_{tr}\,(x_{tr}-2), \tag{20}$$

wherein $x_{tr} \equiv r_{tr}/m$ is an ascending function of $l_{tr} \equiv l\,|_{r=r_{tr}}$. This means that the higher the value of the angular momentum, the further the transition radius from the central object. However, whereas we are interested in investigating the accretion flow in the final instants while the angular momentum must take a lower value compared to the standard Keplerian solution, the matching condition (18) is no longer satisfied. Instead, l behaves as a free parameter, and is responsible for providing the last stages of the accretion-flow condition by taking the value sufficiently lower than l_{tr}.

3. Considering the Equation of State

With the substitution of $V^{(\varphi)}$ (equation 17) in equation (13), there remains just two equations [equations (12)–(13)] and

three variables. Obviously, to close the system it is necessary to include an equation of state. We consider two different equations of state.

3.1. $\bar{p} = K$

Here, K is a constant, which means that if there is no bulk viscosity, the pressure remains constant throughout the fluids' flow. Thus, the continuity and radial-momentum equations [equations (12)–(13)] take the form

$$\bar{\rho}\left[\frac{dV^{(r)}}{dr}+\frac{2}{r}V^{(r)}\right]+V^{(r)}\frac{d\bar{\rho}}{dr}=\frac{3m}{4\pi c^2}\frac{B_0^2}{r^2}\left(\frac{R}{r}\right)^6 V^{(r)}, \tag{21}$$

$$\bar{\rho}\left(1-\frac{V^2}{c^2}\right)^{-1}\left[\frac{d}{dr}\left(V^{(r)}\right)^2+\frac{2mc^2}{r^2}\left(1-\frac{2m}{r}\right)^{-1}\times\left(1-\frac{\left(V^{(r)}\right)^2}{c^2}\right)-\frac{2L^2}{r^3}\left(1-\frac{2m}{r}\right)\right]+\frac{3m}{4\pi}\frac{B_0^2}{r^2}\left(\frac{R}{r}\right)^6=0, \tag{22}$$

wherein $\bar{\rho}=\rho+\bar{p}/c^2$.

3.2. $\bar{p} = \rho c^2$

For this equation of state, equations (12) and (13) are reduced to

$$2\rho\left[\frac{dV^{(r)}}{dr}+\frac{2}{r}V^{(r)}\right]=\frac{3m}{4\pi c^2}\frac{B_0^2}{r^2}\left(\frac{R}{r}\right)^6 V^{(r)}, \tag{23}$$

$$2\rho\left(1-\frac{V^2}{c^2}\right)^{-1}\left[\frac{d}{dr}\left(V^{(r)}\right)^2+\frac{2mc^2}{r^2}\left(1-\frac{2m}{r}\right)^{-1}\times\left(1-\frac{\left(V^{(r)}\right)^2}{c^2}\right)-\frac{2L^2}{r^3}\left(1-\frac{2m}{r}\right)\right]+2c^2\frac{d\rho}{dr}+\frac{3m}{4\pi}\frac{B_0^2}{r^2}\left(\frac{R}{r}\right)^6=0. \tag{24}$$

Thus, we encounter two sets of coupled non-linear ordinary differential equations; it is so difficult to solve them with the common methods. As a first step, we are interested in solving the equations in the special case of no magnetic field being present.

4. Special Case $B_0 = 0$

4.1. $\bar{p} = K$

Equations (21) and (22) are simplified to

$$\frac{d\ln V^{(r)}}{dr}+\frac{2}{r}=-\frac{d\ln\bar{\rho}}{dr}, \tag{25}$$

$$\frac{d}{dr}\left(V^{(r)}\right)^2-\frac{2m}{r^2}\left(1-\frac{2m}{r}\right)^{-1}\left(V^{(r)}\right)^2=-\frac{2mc^2}{r^2}\left(1-\frac{2m}{r}\right)^{-1}+\frac{2L^2}{r^3}\left(1-\frac{2m}{r}\right). \tag{26}$$

Integrating them yields

$$V^{(r)}=\sqrt{\frac{2mc^2}{r}-\frac{L^2}{r^2}\left(1-\frac{2m}{r}\right)}, \tag{27}$$

$$\bar{\rho}=K_1\Big/\left[r^2\sqrt{\frac{2mc^2}{r}-\frac{L^2}{r^2}\left(1-\frac{2m}{r}\right)}\right]. \tag{28}$$

Thus, we have the following relation for the physical density:

$$\rho=\bar{\rho}-\frac{\bar{p}}{c^2}=\frac{K_1}{r^2\sqrt{\frac{2mc^2}{r}-\frac{L^2}{r^2}\left(1-\frac{2m}{r}\right)}}-\frac{K}{c^2}, \tag{29}$$

wherein K_1 and K are constants. The generalized definition for the rate of accretion, $\dot{M}$, in relativity (Bhaskaran & Prasanna 1990) is

$$\dot{M}=\left(\rho+\frac{\bar{p}}{c^2}\right)\left(1-\frac{2m}{r}\right)\left(1-\frac{V^2}{c^2}\right)^{-1}r^2\,V^{(r)}. \tag{30}$$

As infered from equation (29), K_1 will be the rate of accretion, i.e., $K_1=\dot{M}$ and

$$K=p_R-\eta_b\Theta|_{r=R}. \tag{31}$$

Note that it is assumed that the hydrostatic gas pressure at the inner edge is equal to the radiation pressure [$p_R=\frac{1}{3}a\,T^4$ in the local thermodynamical equilibrium (LTE)] (Prasanna 1989). To complete the definitions, it is necessary to expand Θ:

$$\Theta=u^k_{;k}=u^r_{,r}+\frac{2}{r}u^r=\frac{u^0_{,r}}{c}V^r+\frac{u^0}{c}V^r_{,r}+\frac{2}{r}\frac{u^0}{c}V^r, \tag{32}$$

wherein

$$u^0=\left(1-\frac{2m}{r}\right)^{-1/2}\left(1-\frac{V^2}{c^2}\right)^{-1/2} \tag{33}$$

and

$$u^0_{,r}=u^0\left[\left(1-\frac{V^2}{c^2}\right)^{-1}\frac{V}{c^2}\frac{dV}{dr}-\frac{m}{r^2}\left(1-\frac{2m}{r}\right)^{-1}\right]. \tag{34}$$

Also, the fluid total velocity is defined as

$$V^2=(V^{(r)})^2+(V^{(\varphi)})^2=\frac{2mc^2}{r}. \tag{35}$$

Eventually, Θ can be written as

$$\Theta=\frac{u^0}{c}\left\{V^{(r)}\left[\left(1-\frac{V^2}{c^2}\right)^{-1}\left(1-\frac{2m}{r}\right)\frac{V}{c^2}\frac{dV}{dr}+\frac{2}{r}\left(1-\frac{2m}{r}\right)+\frac{m}{r^2}\right]+V^{(r)}_{,r}\left(1-\frac{2m}{r}\right)\right\}, \tag{36}$$

so the following pressure is achieved:

$$p=\bar{p}+\eta_b\Theta=K+\eta_b\Theta. \tag{37}$$

To determine K, it is necessary to assign an appropriate temperature to the marginally stable orbit. Observations have shown that at essentially subcritical fluxes of $\dot{M}=10^{-12}$–$10^{-10}\,M_\odot\,\mathrm{yr}^{-1}$, the luminosity of the disk is of the order of $L=10^{34}$–$10^{36}\,\mathrm{erg\,s}^{-1}$, and the maximal surface temperatures are on the order of $T_s=3\times10^5$–$10^6\,K$ in the inner regions of the disk where most of the energy is released (Shakura & Sunyaev 1973). Therefore, assigning these numerical values for our calculations should not be an odd choice: $M=4\,M_\odot$, $\dot{M}=10^{-12}M_\odot\,\mathrm{yr}^{-1}$ and $T=10^5\,K$ in the inner edge located at

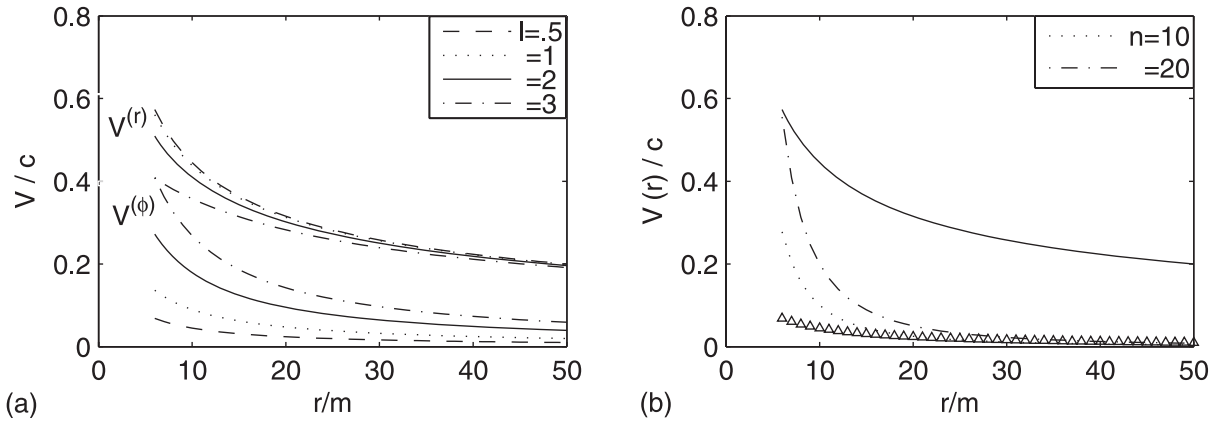

Fig. 1. (a) Velocity profiles of the $\bar{p} = K$ equation of state for different values of l. (b) Azimuthal velocity ('Δ'-marked line) and radial velocity (solid line indicates $\bar{p} = K$ and dotted lines indicate $\bar{p} = \rho c^2$ equation of state for two values of n represented in legend) profiles in the case of $l = 0.5$ and $R = 6m$.

$R = 6m$. Close to the black hole event horizon, the gas temperature and the velocities become extremely high (Popham & Gammie 1998) and gradually fall off outwards (figure 1a). As l increases, the fluids' rotation speeds up, whereas the radial inflow slows down; consequently, the total fluid velocity remains constant with respect to l. Furthermore, as figure 1a clearly shows, l increasing makes the slope of the azimuthal velocity profile steep, and that of the radial velocity profile gentle. Namely, in the process of ascending the velocities inward, an increase in l speeds up this process for the azimuthal velocity and slows it down for the radial velocity. Neglecting the shear viscosity as an angular-momentum transport mechanism necessitates a small gradient for the fluids' azimuthal velocity (Frank et al. 1992). This exerts an upper bound on l, since beyond $l = 1$ the gradient becomes significant.

4.2. $\bar{p} = \rho c^2$

In this equation of state, equations (23) and (24) for the non-magnetofluid reduce to

$$\frac{d \ln V^{(r)}}{dr} = -\frac{2}{r}, \tag{38}$$

$$\frac{1}{c^2 - V^2}\left[\frac{d}{dr}\left(V^{(r)}\right)^2 + \frac{2mc^2}{r^2}\left(1 - \frac{2m}{r}\right)^{-1}\left(1 - \frac{\left(V^{(r)}\right)^2}{c^2}\right) - \frac{2L^2}{r^3}\left(1 - \frac{2m}{r}\right)\right] = -\frac{d \ln \rho}{dr}. \tag{39}$$

Integrating equation (38) gives

$$V^{(r)} = n\,\frac{m^2}{r^2}\,c, \tag{40}$$

wherein n is a free parameter. The radial inflow velocity (dotted lines in figure 1b) becomes faster inward, as in the case of the previous model (subsection 4.1). However, the descending slope of its profile is so much steeper that it falls off rapidly, and reaches to zero, whereas for the $\bar{p} = K$ model it remains constant after an initial gentle infall. The radial velocity in the $\bar{p} = \rho c^2$ model is both independent of l and slower compared with the other model. Furthermore, the upper bound for l is lower. Since l exceeds 0.5, the azimuthal velocity becomes higher than the radial velocity, such that it disturbs the accretion-flow condition during the last stages. Moreover, beyond $r = 20m$ there is neither radial inflow nor rotation for the fluids, and thus the accretion region's vastness for this state is more bounded. Substituting $V^{(r)}$ in equation (39) and integrating yields

$$\rho = \rho_0 \frac{r^4 - m^2 l^2 r^2 + 2m^3 l^2 r - n^2 m^4}{r^3 (r - 2m)}, \tag{41}$$

wherein ρ_0 is the integration constant. Obtaining the density means identifying the pressure via

$$p = \bar{p} + \eta_b \Theta = \rho c^2 + \eta_b \Theta, \tag{42}$$

in which Θ has its previous definition (36); however, the fluid total velocity is changed as

$$V^2 = (V^{(r)})^2 + (V^{(\varphi)})^2 = n^2 \frac{m^4}{r^4} c^2 + \frac{L^2}{r^2}\left(1 - \frac{2m}{r}\right). \tag{43}$$

Increased value of n leads to diminishing the density; for this reason there exists an upper bound for n for which the density and pressure are meaningful. Figure 2 shows the effect of η_b on the pressure and density distributions for two equations of state. The density and pressure for both equations of state are descending functions of r; however, the slope of the density profile for the $\bar{p} = K$ equation of state is steeper in the sense that it drops to zero quickly, whereas for the $\bar{p} = \rho c^2$ model it tends to be constant after an initial falling. The behaviors of the density and pressure distributions in the $\bar{p} = \rho c^2$ model are similar, however, for the other state, unlike the density which falls off rapidly outwards, the pressure remains constant after an initial decrease. With respect to η_b, two equations of state express similar behaviors for the density and different ones for the pressure. The distributions of the density and velocities are not affected by the viscosity parameter. However, regarding the pressure distribution, in the $\bar{p} = K$ model (figure 2a) the higher is the value of η_b, the lower is the value of the pressure in the outer regions, while the pressure descent outward is appreciable only for a high η_b. Also, if there is no bulk viscosity the pressure remains constant throughout the fluids' flow. Extending the marginally stable orbit beyond $R = 6m$

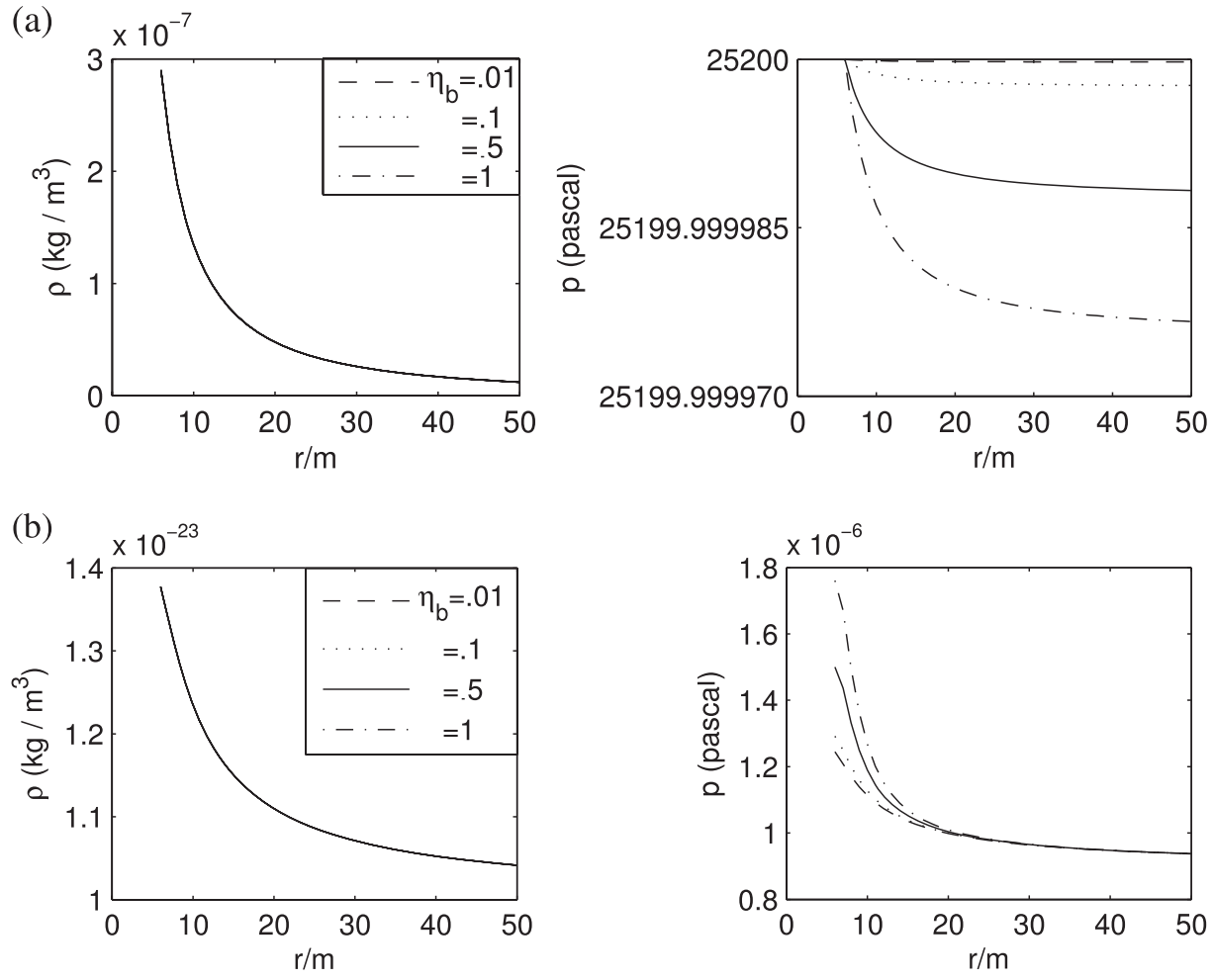

Fig. 2. Density and pressure profiles for different values of η_b for (a) $\bar{p} = K$ and (b) $\bar{p} = \rho c^2$ equation of state. In the case of $R = 6m$, $l = 0.5$, $n = 10$, and $\rho_0 = 10^{-23}\,\mathrm{kg\,m^{-3}}$. The values of η_b are given in the legend.

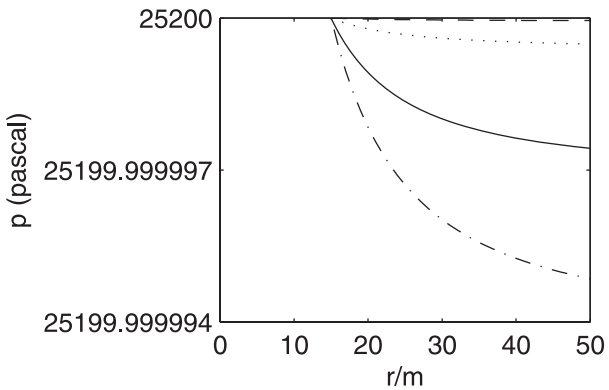

Fig. 3. Same as figure 2a but for $R = 15m$.

(figure 3) leads to increasing the pressure. This increase is significant only for a high η_b. Incidentally, the descending slope of the pressure profile becomes more gentle.

However, for the $\bar{p} = \rho c^2$ equation of state, an increase in η_b results in increasing the pressure in the inner regions (figure 2b). The pressure relation (equation 42) consists of two non-constant terms. Therefore, the pressure continuously maintains the descending outward distribution, even in the case of a vanishing bulk viscosity coefficient, contrary to the $\bar{p} = K$ model. The role of the viscosity term in the pressure ($\eta_b \Theta$) are considered once the two terms are of the same order. Accordingly, the integration constant, ρ_0, is chosen to be $\rho_0 = 10^{-23}\,\mathrm{kg\,m^{-3}}$, so that the effect of viscosity is observed on the pressure distribution. In fact, for densities higher than this value the importance of the bulk viscosity is negligible; however, for the lower densities, the presence of this parameter is more noticeable.

In the allowed interval for l, the density and pressure distributions for both states do not vary to an appreciable extent against l. Nevertheless, once l exceeds this limit, the density and pressure increase with l increasing in the $\bar{p} = K$ the equation of state, and decrease for the other state. Owing to the fact that this behaviour is beyond the physical limit for l, the profiles have not been plotted.

5. General Case $B_0 \neq 0$

The solutions to Maxwell's equations [equations (10)]

indicate on dipolar configuration for electromagnetic fields which could match for the modelling of accretion disks around neutron stars. Thus, in this case the central compact object is assumed to be a pulsar with mass $M = M_\odot$ and radius $R = 6m$. Though it may be rotating in general, the Schwarzschild geometry is used to describe the space-time curvature. This is because it is assumed that the angular-momentum parameter is $a \ll 1$, which indeed seems to be the case for most pulsars (e.g., Gonthier & Harding 1994; Banerjee et al. 1997). Since the solutions of the magnetofluid case must be the previous ones in case $B_0 = 0$, we choose the solutions of the equations in the latter case to be exactly the same as before, plus terms involving B_0, which must be vanished once $B_0 = 0$. For the magnetized case, we don't discuss the $\bar{p} = K$ equation of state. This is because this state demands that the pressure balance at the inner edge is mainly provided by equality of the hydrostatic gas pressure and the magnetic pressure instead of the radiation pressure. Therefore, K becomes so much larger than the second term ($\eta_b \Theta$) in the pressure equation (37), and the pressure remains constant throughout the accretion flow, whereas the density increases inward as before, which seems to be an unreasonable result. For the $\bar{p} = \rho c^2$ equation of state, the solutions of equations (23) and (24) are presumed to be as follows:

$$V^{(r)} = n\frac{m^2}{r^2}c - \frac{B_0^2}{P_m}c\,g\left(\frac{r}{m}\right), \tag{44}$$

$$\rho = \rho_0 \frac{r^4 - m^2 l^2 r^2 + 2m^3 l^2 r - n^2 m^4}{r^3(r-2m)} - \frac{B_0^2}{c^2} f\left(\frac{r}{m}\right), \tag{45}$$

where g and f are dimensionless functions that are determined by solving equations (23) and (24) numerically. P_m, which is the average magnetic pressure throughout the accretion flow, is a constant employed in the equations to fit the additional magnetic terms from a dimensional point of view. It is defined as

$$P_m = \frac{< B^2 >}{8\pi}$$

$$= \frac{1}{8\pi}\frac{1}{(r_2 - r_1)}\int_{r_1 = R_M = 10m}^{r_2 = 50m}\left(B_{(r)}^2 + B_{(\theta)}^2 + B_{(\varphi)}^2\right)dr$$

$$= 2.787 \times 10^{11}\ \text{pascal}. \tag{46}$$

Here, R_M is the radius of the inner edge, where inside it the matter flows along field-lines (Frank et al. 1992). We choose a negative sign for the magnetic terms in equations (44) and (45) since, as we know, the presence of a magnetic field in the fluids is a decelerating factor in the sense that the flow of the magnetofluid is stopped by the magnetic pressure associated with a compact object (Tripathy et al. 1990). The pressure is obtained from equation (42) once more, but with a new definition for the radial velocity [equation (44)]. The appearance of the magnetic field in the system slows down the radial inflow; however, doesn't affect the angular-momentum distribution. As the magnetic field strengthens, the radial inflow both becomes slower and its slope becomes more gentle (figure 4). The provision of accretion flow in the last stages puts an upper

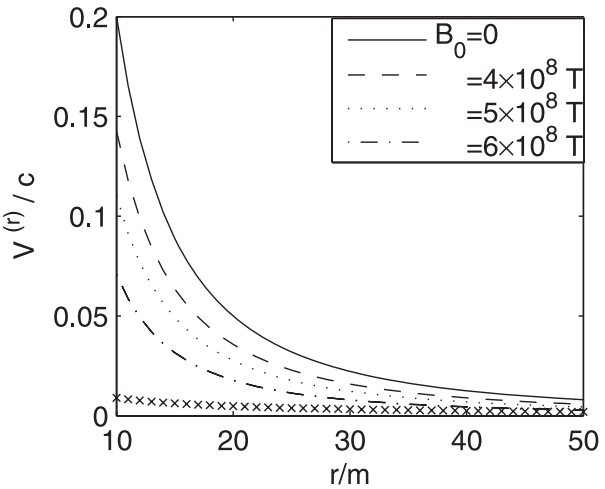

Fig. 4. Radial velocity profile of the magnetofluid for different values of B_0, in the case of $n = 20$, $l = 0.1$, and $\bar{p} = \rho c^2$ equation of state. The '$\times\ \times$' sign represents $V^{(\varphi)}$ profile. The values of B_0 are represented in the legend.

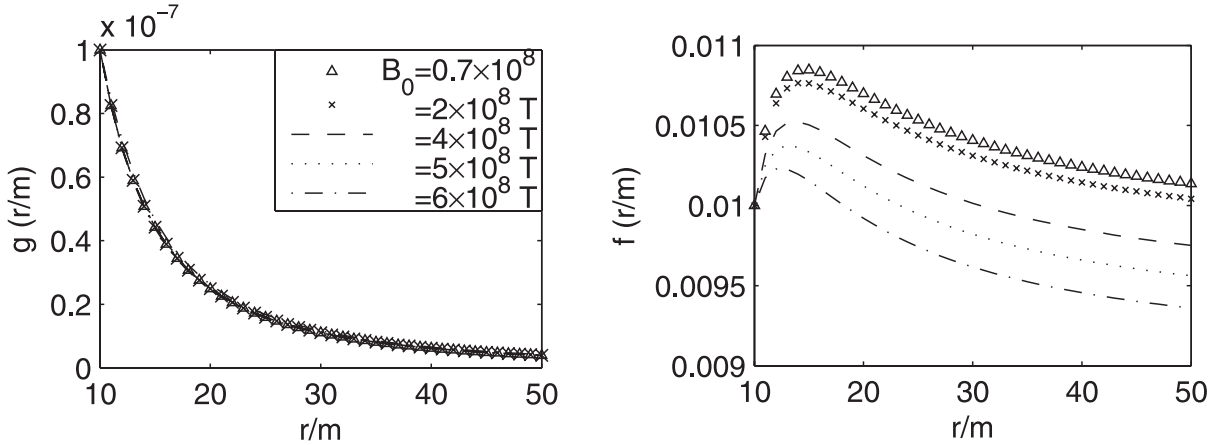

Fig. 5. g and f profiles of the magnetofluid for different values of B_0. The values of B_0 are represented in the legend.

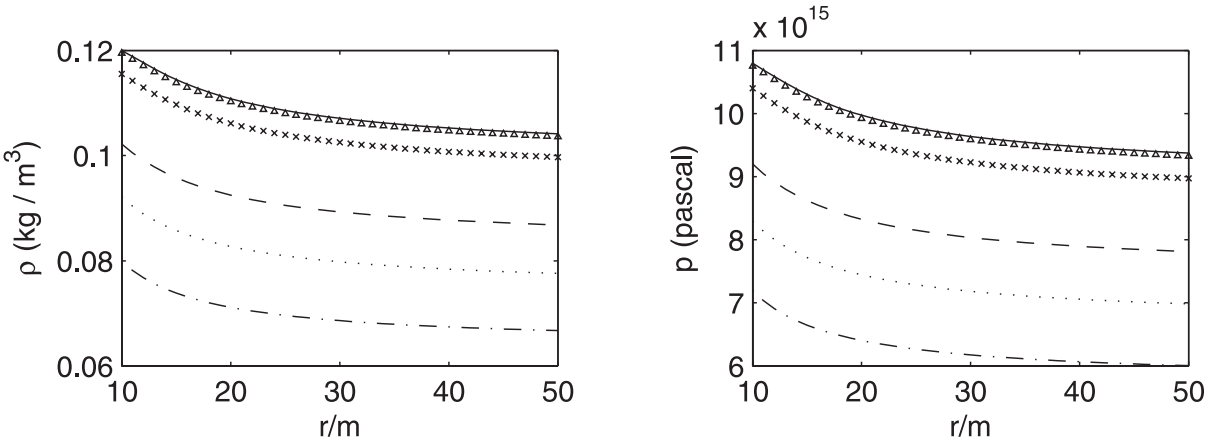

Fig. 6. Density and pressure profiles of the magnetofluid for different values of B_0 for the $\bar{p} = \rho c^2$ equation of state, in the case of $n = 20$, $l = 0.1$, and $\rho_0 = 0.1\,\mathrm{kg\,m^{-3}}$. The values of B_0 are represented in the legend of figure 5.

limit on the value of B_0, the surface magnetic field of the central neutron star. This is because at those instants the radial inflow must be so faster than the azimuthal velocity.

Figure 5 gives the profiles of dimensionless functions g and f for different values of B_0. As one can see, g is not affected by B_0, whereas f decreases as B_0 increases. Further, figure 6 shows the effect of B_0 on the density and pressure distributions. As expected, the density as well as the pressure fall off as the magnetic field strengthens. There exists a lower bound on the value of ρ_0 below which the density and pressure become negative (due to presence of magnetic terms with negative sign), and hence leads to an unphysical situation.

6. Conclusion

We have written the equations describing the viscous accreting magnetofluids around a static compact object in the final stages of accretion flow, and solved them not only in the special case of electromagnetic field absence, but also in the case of a plasma disk in the presence of a dipole magnetic field. We have achieved two sets of solutions for two different equations of state in the non-magnetofluid case. The density and pressure for both states ascend inward. The increasing density at the inner regions during the last phases of accretion flow suggests that the inner regions could be blown up with matter moving along the θ direction on either side of the equatorial plane. The accretion-flow condition during the last stages demands that the fluids' radial inflow is carried out much faster than its rotation. In those situations, there is no need for any angular-momentum transport mechanism; therefore, one may neglect the shear viscosity. Elimination of the shear viscosity coefficient, η_s, both simplifies the equations and exerts an upper limit on the angular-momentum parameter, l. Because a small gradient of the angular velocity is incidental to vanishing the shear viscosity, and since an increase of l makes the slope of the azimuthal velocity steeper, there should be an upper bound on it. This upper limit for the $\bar{p} = \rho c^2$ equation of state is lower than the other state. Thus, the $\bar{p} = K$ model can support a higher value of the azimuthal velocity against the $\bar{p} = \rho c^2$ model. In any case, for both states it is much slower than the standard Keplerian solution. The results that we have attained for the non-magnetofluids surrounding a static black hole in the case of the $\bar{p} = K$ equation of state from the viewpoint of the qualitative behavior of the physical functions are just the same as whatever has been achieved for fluids around a rotating compact object, whose angular velocity is essentially due to dragging originating from the surrounding space-time (Prasanna 1989).

The accreting plasma in the presence of a dipole magnetic field gives rise to a current in the azimuthal direction and a charge density, J^t. However, this current doesn't generate a new magnetic field, because of a loss of the electrical conductivity. Consequently, the dipolar configuration of the central pulsar magnetic field isn't disturbed (Prasanna et al. 1989; Tripathy et al. 1990). The relativistic magnetohydrodynamical equations describing the plasma have been resolved by employing solutions obtained from their hydrodynamical peers. In order to ensure that the density and pressure are positive everywhere, the free parameter ρ_0 should not be lower than $0.1\,\mathrm{kg\,m^{-3}}$. Under these circumstances, the term ρc^2 will be much greater than that of $\eta_b \Theta$, and dominates over it. As a consequence, no longer does the bulk viscosity affect the pressure distribution. Indeed, with the appearance of electromagnetic fields in the fluids, it seems that the bulk viscosity doesn't have the previous importance on the dynamics, Bhaskaran and Prasanna (1990) also note this point.

In conclusion, the solutions that we have examined here for accreting fluids confined to the equatorial plane of a non-rotating compact object may be important in this respect: By incorporating the effects of other feasible parameters, like shear viscosity, heat conduction and resistivity, these solutions can be used plus the terms including the relevant coefficients (i.e., η_s shear viscosity or χ heat conduction coefficient and σ conductivity), analogous to what we have done by taking into account the electromagnetic fields.

To generalize the problem, it is interesting to put aside the assumptions of the fluids' equatorial plane confinement and no meridional flow. We will address this problem in a forthcoming paper.

References

Antón, L., Zanotti, O., Miralles, J. A., Martí, J. M., Ibáñez, J. M., Font, J. A., & Pons, J. A. 2006, ApJ, 637, 296
Banerjee, D., Bhatt, J. R., Das, A. C., & Prasanna, A. R. 1995, ApJ, 449, 789
Banerjee, D., Bhatt, J. R., Das, A. C., & Prasanna, A. R. 1997, ApJ, 474, 389
Bhaskaran, P., & Prasanna, A. R. 1990, J. Astrophys. Astron., 11, 49
Cai, M. J., & Shu, F. H. 2002, ApJ, 567, 477
Frank, J., King, A., & Raine, D. 1992, Accretion Power in Astrophysics (Cambridge: Cambridge University Press)
Gammie, C. F., McKinney, J. C., & Tóth, G. 2003, ApJ, 589, 444
Ghosh, P. 2000, MNRAS, 315, 89
Gonthier, P. L., & Harding, A. K. 1994, ApJ, 425, 767
Kaburaki, O. 1986, MNRAS, 220, 321
Kudoh, T., & Kaburaki, O. 1996, ApJ, 460, 199
Lynden-Bell, D., & Pineault, S. 1978, MNRAS, 185, 695
Peitz, J., & Appl, S. 1997, MNRAS, 286, 681
Popham, R., & Gammie, C. F. 1998, ApJ, 504, 419
Prasanna, A. R. 1989, A&A, 217, 329
Prasanna, A. R., & Bhaskaran, P. 1989, Ap&SS, 153, 201
Prasanna, A. R., Tripathy, S. C., & Das, A. C. 1989, J. Astrophys. Astron., 10, 21
Riffert, H. 2000, ApJ, 529, 119
Shakura, N. I., & Sunyaev, R. A. 1973, A&A, 24, 337
Takahashi, M., Nitta, S., Tatematsu, Y., & Tomimatsu, A. 1990, ApJ, 363, 206
Tomimatsu, A., & Takahashi, M. 2001, ApJ, 552, 710
Tripathy, S. C., Prasanna, A. R., & Das, A. C. 1990, MNRAS, 246, 384